The Role of Macrophages in Early Healing of a Tendon Graft in a Bone Tunnel

By Peyton L. Hays, MD, Sumito Kawamura, MD, Xiang-Hua Deng, MD, Elias Dagher, MD, Kai Mithoefer, MD, Liang Ying, BS, and Scott A. Rodeo, MD

Investigation performed at The Laboratory for Soft Tissue Research, The Hospital for Special Surgery, New York, NY

Background: Macrophages accumulate following tendon-to-bone repair and may contribute to the formation of a scar-tissue interface rather than to the reformation of a normal insertion site. We hypothesized that macrophage depletion may lead to improved insertion site regeneration, in a form of ''scar-less'' healing rather than reactive scar-tissue formation.

Methods: One hundred and ninety-two Sprague-Dawley rats underwent anterior cruciate ligament reconstruction with use of a flexor tendon autograft and were divided into a control group (ninety-six rats) and a liposomal clodronate-injected group (ninety-six rats). Clodronate is a bisphosphonate that selectively induces macrophage apoptosis. Animals in the liposomal clodronate group received weekly intraperitoneal injections of liposomal clodronate (1.33 mL/100 g of body weight). Rats were killed at serial time points from three to forty-two days. Immunostaining identified macrophages and transforming growth factor-beta (TGF-β) at the tendon-bone interface. Fibrous interface width, osteoid formation, and collagen fiber continuity were evaluated with use of histomorphometry. Serial fluorochrome labeling was used to measure mineral apposition rate. Additional rats were killed for biomechanical testing at seven, fourteen, twenty-eight, and forty-two days.

Results: Liposomal clodronate significantly decreased macrophages and TGF-β accumulation at the tendon-bone interface ($p < 0.05$). Specimens from rats that received liposomal clodronate exhibited a significantly narrower fibrous tissue interface between tendon and bone at all time points compared with specimens from controls ($p < 0.05$). In specimens from the liposomal clodronate group, healing proceeded at an accelerated rate, characterized by enhanced collagen fiber continuity and a greater degree of interface remodeling between tendon and bone. There were significant increases in osteoid formation ($p < 0.05$) and mineral apposition rates ($p < 0.05$) among experimental specimens. At forty-two days, the specimens from the liposomal clodronate group had significantly greater increases than the control specimens with respect to load to failure (mean and standard deviation, 13.5 ± 4.2 N and 9.7 ± 3.9 N, respectively; $p < 0.05$) and stiffness (mean, 11.5 ± 5.0 N/mm and 7.5 ± 3.2 N/mm; $p < 0.05$).

Conclusions: Macrophage depletion following anterior cruciate ligament reconstruction resulted in significantly improved morphologic and biomechanical properties at the healing tendon-bone interface, which we hypothesize are due to diminished macrophage-induced TGF-β production.

Clinical Relevance: Techniques to modulate inflammation, and specifically macrophages, may improve tendon-bone healing and may enhance the structural integrity of healing tendon grafts.

Anterior cruciate ligament reconstruction with use of a tendon graft placed through bone tunnels is a commonly performed orthopaedic procedure[1]. Despite generally favorable results with anterior cruciate ligament reconstruction, instrumented testing of knee stability demonstrates frequent increased anterior laxity, which may lead to symptomatic instability[2]. Long-term outcome studies have found increases in joint laxity over time[3-5]. Although many factors, including graft fixation, initial graft tension, graft material, and postoperative rehabilitation, determine the

Disclosure: The authors did not receive any outside funding or grants in support of their research for or preparation of this work. Neither they nor a member of their immediate families received payments or other benefits or a commitment or agreement to provide such benefits from a commercial entity. No commercial entity paid or directed, or agreed to pay or direct, any benefits to any research fund, foundation, division, center, clinical practice, or other charitable or nonprofit organization with which the authors, or a member of their immediate families, are affiliated or associated.

outcome of anterior cruciate ligament reconstruction, one of the most important factors is graft healing to bone. Failure of secure healing of the tendon in the bone tunnel prior to return to activity can result in graft slippage in the tunnel with resultant increased knee motion.

Successful ligament reconstruction in the knee with use of a tendon graft depends on secure tendon-to-bone healing. The native ligament insertion site is a highly specialized transition zone that functions in the transmission of mechanical load from soft tissue to bone[6]. The normal insertion site is approximately 1 mm in length and consists of four distinct regions: ligament, unmineralized fibrocartilage, mineralized fibrocartilage, and bone[6,7]. A number of experimental models have shown that the complex structure and composition of the normal insertion site are not regenerated following ligament reconstruction[6-13]. Healing in these models occurs by formation of a fibrovascular "scar" tissue interface rather than reformation of a normal insertion site. This fibrous scar interface lacks the structural integrity of the native attachment site.

We used a rat model of anterior cruciate ligament reconstruction, in which an autogenous flexor tendon graft is placed through drill-holes in the femur and the tibia, to study tendon graft-healing in a bone tunnel. We found that healing begins with an early influx of inflammatory cells followed by the formation of a fibrovascular interface tissue between the tendon graft and bone. As healing proceeds, there is gradual bone ingrowth into the tendon and progressive establishment of collagen fiber continuity between tendon and bone, followed by tissue remodeling and maturation[6-14]. We identified two distinct subpopulations of macrophages that accumulate in the healing tendon-bone interface[11]. Macrophages expressing the ED1 antigen are recruited from circulating blood monocytes, accumulate in the first few days following surgery (peaking at seven days), and have a phagocytic function in débriding the wound environment, while macrophages expressing the ED2 antigen are derived from the local tissue environment, have maximum accumulation by twenty-eight days, and have an anabolic role in tissue healing.

One of the principal functions of macrophages is the secretion of growth factors and cytokines responsible for fibroblast mitogenesis and proliferation, extracellular matrix and collagen synthesis, and angiogenesis[15-19]. Of these cytokines, transforming growth factor-β (TGF-β) is one of the most important mediators of early macrophage activity in normal wound-healing. TGF-β stimulates the synthesis of extracellular matrix components, inhibits the production of tissue proteinases, and increases the production of tissue proteinase inhibitors[15,16,20-24]. We hypothesized that the rapid influx of macrophages and subsequent cytokine production contribute to the early formation of the fibrous scar-tissue interface rather than to the reformation of a normal insertion site.

Further insight into the role of macrophages and other inflammatory cells in scar formation during wound-healing comes from the study of fetal wounds, which heal by tissue regeneration rather than scar formation, in the absence of inflammatory cell infiltrate[14,25,26]. By the late gestation stage, fetal wounds heal by fibrotic scar formation, which corresponds with the appearance of macrophage recruitment[25]. The fetal wound environment has been simulated in vivo by eliminating macrophages or inhibiting TGF-β expression[14,19,27,28]. For example, following venous grafting in macrophage-depleted rats, Wolff et al. observed decreased neointimal hyperplasia and reduced cellularity in the setting of reduced expression of TGF-β1 and macrophage chemotactic protein-1 (MCP-1)[19]. Martin et al. described "scar-less" wound-healing in a mouse knockout model deficient of macrophages and neutrophils[29]. Of note, these wounds healed at the same rate as those in control animals, suggesting that acute inflammation may not be necessary for adequate wound repair. Other studies have focused on the correlation between the level of TGF-β1 expression and fibrous tissue formation during early wound-healing[14,15,21,28,30,31]. Overexpression of TGF-β1 has been used to create experimental models of chronic organ fibrosis[21,31], while strategies to reduce TGF-β1 expression have resulted in decreased extracellular matrix deposition and reduced fibrovascular tissue formation[14,28]. Taken together, these studies have led to our hypothesis that macrophage depletion would result in decreased fibrovascular "scarring" between tendon graft and bone, leading to regeneration of a more normal insertion site, with improved structural integrity, rather than reactive scar formation at the healing insertion site. To test this hypothesis, we evaluated tendon-to-bone healing in rats that had been depleted of macrophages with use of serial injections of a known macrophage-targeting agent, liposome-encapsulated dichloromethylene-bisphosphonate (Cl_2MBP or liposomal clodronate), following anterior cruciate ligament reconstruction. Healing was evaluated with quantitative histomorphometric and biomechanical analyses performed at serial time points.

Materials and Methods

Study Animals

A total of 192 male Sprague-Dawley rats (Harlan, Indianapolis, Indiana), weighing 300 to 350 g, underwent anterior cruciate ligament reconstruction in the right knee with use of an autologous ipsilateral flexor digitorum longus tendon graft. The animals were randomly assigned to one of two groups: the control group (ninety-six rats) or the liposomal clodronate-injected group (ninety-six rats). Animal care was provided according to guidelines established by the Center for Laboratory Animal Services at our institution. Injections were performed without animal sedation. All protocols were approved by the Institutional Animal Care and Use Committee.

Macrophage Depletion by Means of Liposomal Clodronate

To evaluate the role of macrophages in tendon-to-bone healing following anterior cruciate ligament reconstruction, liposomal clodronate was administered to the experimental group to selectively deplete macrophages. Clodronate is a bisphosphonate (Cl_2MBP) commonly used to treat metabolic or malignant bone diseases. When encapsulated within liposomes, it is actively and exclusively phagocytosed by macrophages and induces apoptosis without macrophage stimulation[32]. Liposomes

containing clodronate were obtained from the Clodronate Liposomes Foundation (Vrije Universiteit, VUmc, Amsterdam, The Netherlands). In brief, a mixture of phosphatidylcholine (Lipoid, Ludwigshafen, Germany) and cholesterol (Sigma Chemical, St. Louis, Missouri) was suspended in 0.6-M clodronate (a gift of Roche Diagnostics, Mannheim, Germany) and sonicated to produce multilamellar liposomes[33]. The liposomes were washed twice by ultracentrifugation to remove nonencapsulated clodronate and then were resuspended in phosphate buffered saline solution for injection. Two days prior to surgery, rats in the experimental group were administered 1.33 mL/100 g of liposomal clodronate by intraperitoneal injection. Animals then received weekly injections of the same dose until the time when they were killed[34]. An additional 0.1 mL of liposomal clodronate was injected directly into the knee joint at the time of surgery. Animals were carefully monitored for signs and symptoms of local or systemic infection. Prior work in our laboratory with use of a similar experimental design at a lower dose of liposomal clodronate did not demonstrate an increased incidence of infection[10]. The control animals did not receive injections of liposomes without clodronate, because there is no evidence that the liposomes alone would have any effect on healing.

Surgical Procedure

We used a rat model of anterior cruciate ligament reconstruction that we developed in our laboratory[11]. Animals were sedated by intraperitoneal injection of a mixture of 80 mg/kg of ketamine hydrochloride and 5 mg/kg of xylazine and were maintained under sedation with inhaled isoflurane as necessary. The right hind limb was prepared and draped in sterile fashion. Two 5-mm incisions were made on the medial aspect of the distal part of the leg and the plantar surface of the foot. Dissection of the flexor digitorum longus tendon was carried out at both sites, and the full length of the tendon was harvested. A third incision was made over the knee, and a medial arthrotomy was performed. The native anterior cruciate ligament was excised. With use of an 18-gauge needle (1.27-mm diameter), a bone tunnel was drilled in the proximal aspect of the tibia and the distal part of the femur at the insertion sites of the anterior cruciate ligament. The harvested tendon graft was passed through both bone tunnels. The ends of the tendon graft were secured to the periosteum of the distal aspect of the femur and proximal part of the tibia as well as the collateral ligaments with use of 4-0 Ethibond suture (Ethicon, Somerville, New Jersey). The deep and superficial incisions were closed in routine fashion with use of 4-0 Vicryl (polyglactin) and 4-0 Ethilon suture (Ethicon), respectively. Animals were allowed ad libitum postoperative activity.

Fluorochrome Labeling

Twelve animals in each group were injected with serial fluorochrome labels before they were killed, at seven, fourteen, twenty-eight, and forty-two days, in order to label newly mineralized bone along the bone tunnels. These animals received intraperitoneal injections of 25 mg/kg of calcein (Sigma-Aldrich, St. Louis, Missouri) and 90 mg/kg of xylenol orange (Sigma-Aldrich) at eight and three days, respectively, before they were killed. The seven-day animals received calcein seven days before they were killed and xylenol orange three days before they were killed.

Tissue Preparation

Eight rats in each group were killed by carbon dioxide inhalation at three, seven, ten, fourteen, twenty-eight, and forty-two days following surgery. The involved hind limbs were dissected to the joint capsule, and the femora and tibia were detached. Five specimens from each group were prepared for histologic analysis after decalcification. These samples were fixed in 10% neutral buffered formalin at 4°C for three days. Following fixation, specimens were cut in cross-section perpendicular to the axis of the tendon graft in the bone tunnel with use of a cooled diamond wheel saw and then were decalcified overnight at 4°C in Immunocal (Decal Chemical, Tallman, New York). The tissue was dehydrated in increasing concentrations of alcohol (70% to 100%) and was cleared in three changes of xylene. The tissue was then embedded in paraffin at 60°C. Serial sections that were 5 μm thick were prepared for hematoxylin and eosin staining and immunohistochemistry.

The other three specimens at each time point were prepared for histologic analysis without decalcification. Samples were fixed in 70% ethanol, and coronal sections along the long axis of the tendon graft were cut. The sections were further dehydrated in increasing concentrations of alcohol, were fixed in acetone, and then were embedded in methylmethacrylate. Serial sections that were 5 μm thick were prepared for Goldner-Masson trichrome staining and fluorescence microscopy.

Immunohistochemistry

Immunohistochemistry was used to identify macrophages at the tendon-bone interface. Two distinct subpopulations of macrophages that selectively express ED1 lysosomal glycoprotein antigen or ED2 membrane glycoprotein antigen have been identified[18,35,36]. ED1+ macrophages represent the monocyte-derived population recruited from the circulation to the site of wound-healing, while ED2+ macrophages are those activated and derived from the local microenvironment.

Hydrated serial sections were treated with 3% H_2O_2 to quench endogenous peroxidase activity, and nonspecific antibody binding was blocked with 5% goat serum. Mouse anti-rat antibodies to ED1-macrophages (CD68) and ED2-macrophages (CD163) (Serotec, Raleigh, North Carolina) were used to localize macrophages in the healing tendon-bone interface. We also localized TGF-β using a rabbit polyclonal antibody (Abcam, Cambridge, Massachusetts). Primary antibodies were applied to separate serial sections for sixty minutes at room temperature. Bound antibodies were visualized with use of a goat avidin-biotin peroxidase system with 3,3′-diaminobenzidine (DAB; Dako, Carpinteria, California) as a chromagen. The number of ED1, ED2, or TGF-β-positive cells were counted in

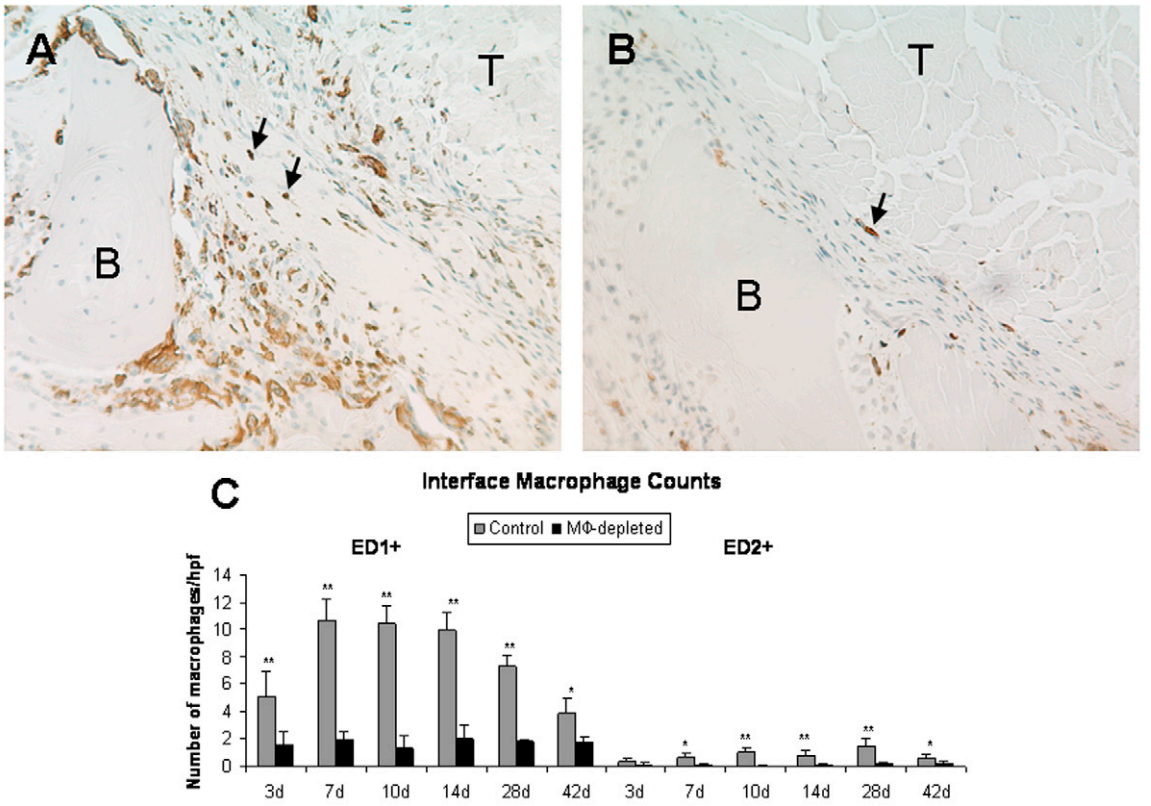

Fig. 1

Immunostaining for the ED1 antigen at the tendon-bone interface of control (A) and macrophage-depleted (B) specimens seven days following anterior cruciate ligament reconstruction (160× magnification). Specimens from animals that had been administered liposomal clodronate exhibited significantly fewer positively staining macrophages (arrows) than control specimens at all time points (C). *$p < 0.05$. **$p < 0.01$. T = tendon, and B = bone.

ten high-power fields (50 μm × 50 μm at 160× magnification) per specimen.

Histologic Analysis

Decalcified histologic sections were stained with hematoxylin and eosin for routine histomorphologic analyses with use of a light microscope (Nikon Optiphot; Nikon USA, Melville, New York) connected to a charge coupled device (CCD) camera (Nikon DXM1200; Nikon USA). The histologic sections were reviewed by two authors (P.L.H. and S.A.R.) who were blinded to the group, and the final grade was determined by consensus. Locations along the perimeter of the tendon-bone interface were systematically selected, and the width of fibrovascular tissue formation between tendon and bone was measured (160× magnification). All histomorphometric assessments were made with use of ImageJ software (National Institutes of Health, Bethesda, Maryland). We first examined the tibial and femoral tunnel data separately and found no differences between the two tunnels. The data for the tibial and femoral tunnels were thus combined.

Decalcified sections were also stained with picrosirius red staining and then were examined under polarized light to optimize visualization of collagen fiber continuity between graft and bone[37,38]. The polarizer was rotated to the position of maximum birefringence (brightness) on each slide. The light intensity on the microscope was kept constant for all specimens to standardize the measurements and reduce the potential for error. Ten randomly selected digital images were collected for each specimen. With use of ImageJ software, the images were converted to 8-bit grayscale on which the brightness of individual pixels was represented on a scale from 0 to 255, with 255 indicating maximum pixel brightness. Average brightness per high power field (50 μm × 50 μm at 320× magnification) was measured at several randomly chosen locations along the tendon-bone interface for each image. The brightness is proportional to collagen fiber density and organization.

We identified newly mineralized bone along the bone tunnels in the fluorochrome-labeled sections. Unstained coronal sections were observed under fluorescent light, and digitized images were recorded along the length of the tendon graft-bone tunnel interface (320× magnification). The distance between fluorochrome labels was measured, and the mineral apposition rate was determined. Serial coronal sections were also stained with Goldner-Masson trichrome stain for quantitative analysis of new osteoid formation at the tendon-bone interface. The thickness of the "seam" of newly deposited os-

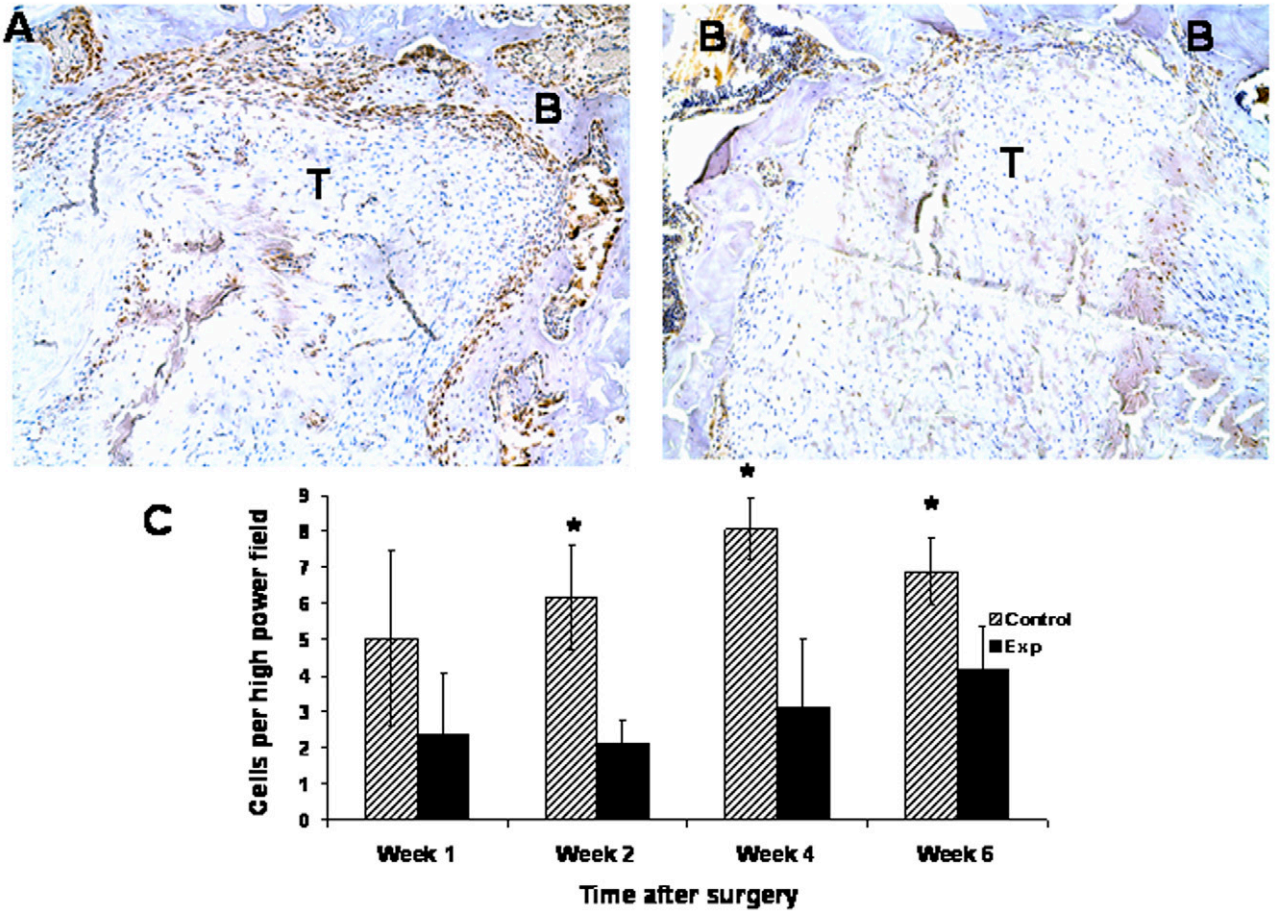

Fig. 2

Immunostaining for TGF-β-positive macrophages at the tendon-bone interface of control (A) and macrophage-depleted (B) specimens at twenty-eight days following anterior cruciate ligament reconstruction. There were significantly fewer TGF-β-positive cells in the macrophage-depleted specimens compared with the control limbs at all time points tested (C). Positive cells stain brown. *$p < 0.01$. T = tendon, and B = bone.

teoid along the bone tunnel was measured with use of ImageJ software (320× magnification). Because the precision of these measurements requires accurate coronal plane sections, we ensured reproducible sectioning by identifying the tunnel entrance and exit, which facilitates accurate sectioning in the coronal plane.

Biomechanical Testing

Twelve rats in each group were killed for biomechanical testing at seven, fourteen, twenty-eight, and forty-two days following surgery. The femur-anterior cruciate ligament graft-tibia construct was harvested and frozen at –80°C until testing. Prior to testing, all soft tissue was dissected leaving the anterior cruciate ligament graft. The tibiae and femora were potted in cement to ensure secure fixation. Specimens were mounted on a materials testing machine (MTS Systems, Eden Prairie, Minnesota) in a specially designed jig so that tension was aligned along the long axis of the tendon graft. A preload of 0.2 N was applied, and then the specimens were preconditioned for five cycles. The specimens were then loaded in uniaxial tension to graft failure. Load to failure (N) and stiffness (N/mm) were determined from the linear portion of the load-deformation curve with use of SigmaPlot 8.0 (SPSS, Chicago, Illinois). The site of graft failure (pullout from bone tunnel compared with midsubstance rupture) was also recorded.

Statistical Methods

The data were compared between groups with use of the Wilcoxon rank-sum test and unpaired t tests. Biomechanical failure mode was analyzed with use of the chi-square test for independence. Differences were considered significant at $p < 0.05$. All data are presented as the mean and the standard error of the mean.

Results

Animal Model

The surgical procedure was well tolerated with few complications. Three intraoperative deaths (two in the control group and one in the experimental group) and one early postoperative death (control group) occurred secondary to complications with anesthesia. Two animals (both in the experimental group) were killed early because of dehiscence of the surgical

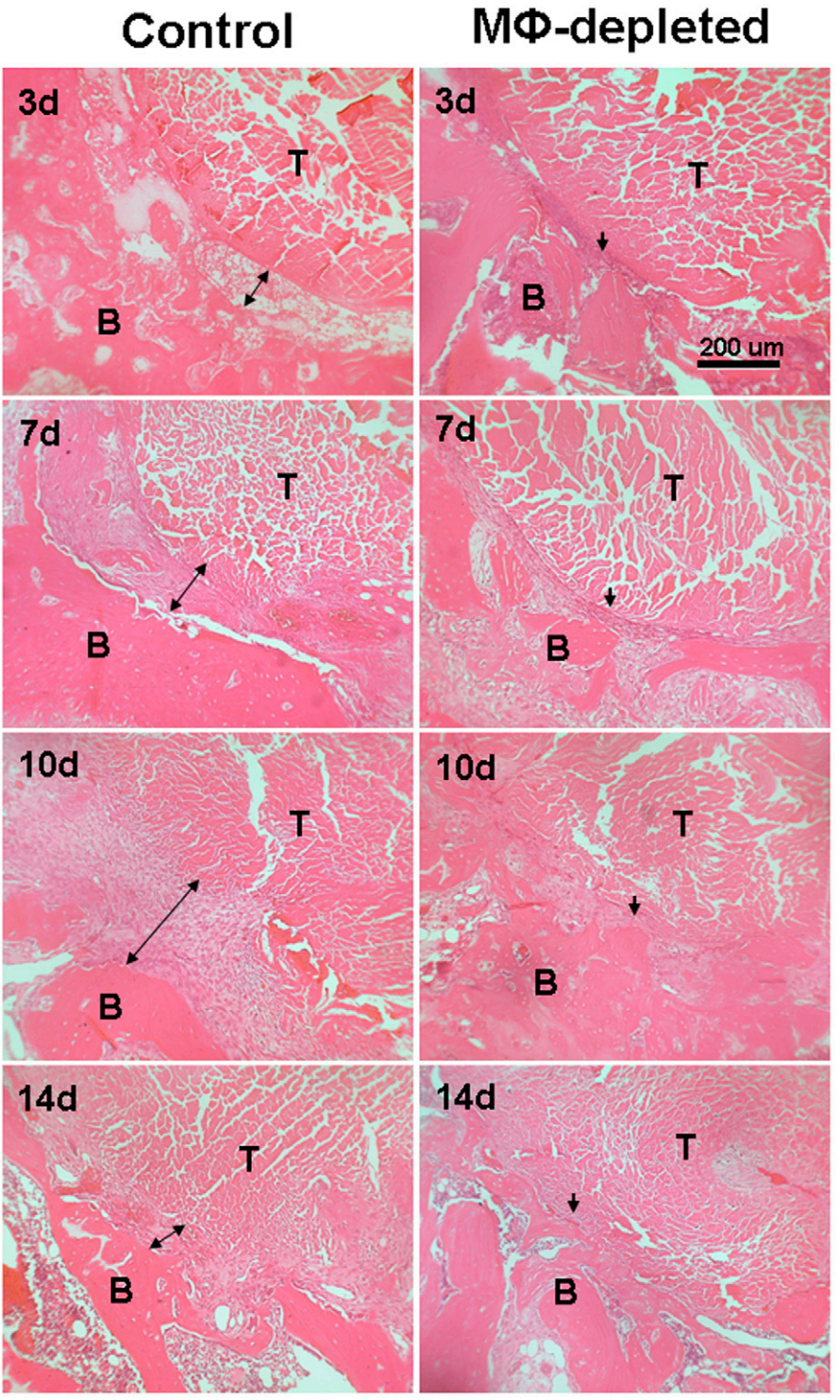

Fig. 3-A

Early healing at the tendon-bone interface consisted of the formation of a poorly organized fibrous tissue interface between tendon graft and bone. As healing progressed, the interface tissue became more organized with gradual integration of the surrounding bone and tendon. Among macrophage-depleted specimens, healing proceeded at an accelerated rate with earlier establishment of collagen fiber continuity and improved organization of the fibrous interface tissue compared with controls. Interface tissue widths are illustrated by arrows (hematoxylin and eosin, ×80). T = tendon, and B = bone.

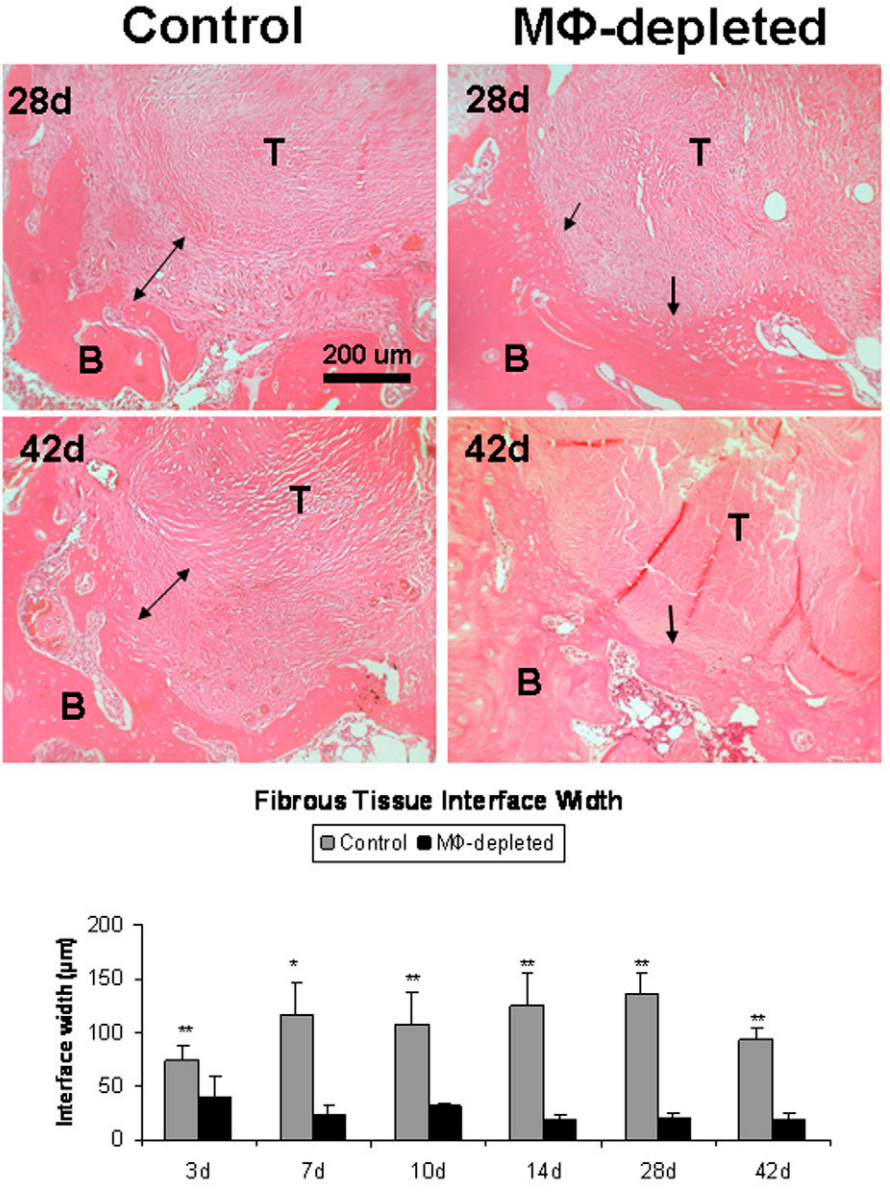

Fig. 3-B

At twenty-eight and forty-two days, interface remodeling continued among control and macrophage-depleted specimens with greater morphologic change among the latter group. By forty-two days, the tendon-bone interface in the macrophage-depleted specimens was characterized by frequent regions of fibrocartilaginous transition between tendon and bone (hematoxylin and eosin, ×80). At all time points, the width of fibrous tissue interface was significantly reduced following macrophage depletion. *$p < 0.05$. **$p < 0.01$. T = tendon, and B = bone.

incision secondary to the animal chewing at the site. All prematurely killed animals were replaced as per protocol. No adverse clinical observations were noted as a result of the liposomal clodronate injections. There were no deep infections.

Presence of ED1+ and ED2+ Macrophages at the Healing Tendon-Bone Interface

ED1+ macrophages were observed as part of the early inflammatory cell infiltrate at the tendon graft-bone interface at three days following surgery among control specimens (5.1 ± 1.8 cells per high-power field; Fig. 1). By seven days, the number of ED1+ macrophages had doubled to 10.7 ± 1.6 cells per high-power field. Over the remaining time points, the presence of ED1+ macrophages at the tendon-bone interface among control specimens slowly declined to 3.9 ± 1.1 cells per high-power field at forty-two days. In contrast, very few ED2+ cells were observed throughout the early postoperative time points among control animals, ranging from 0.3 ± 0.3 cells per

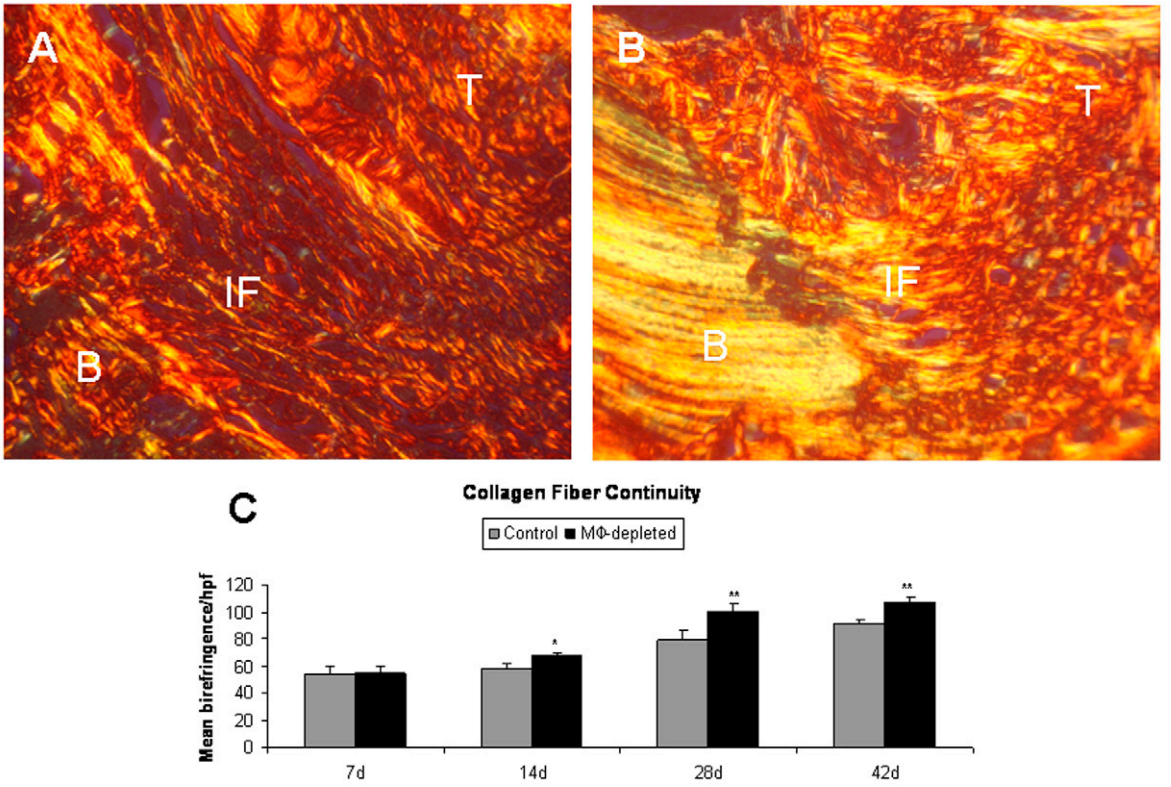

Fig. 4

Polarized light images of the tendon-bone interface of control (A) and macrophage-depleted specimens (B) at forty-two days. Macrophage depletion resulted in enhanced collagen fiber continuity and greater mean collagen fiber birefringence at the interface between tendon graft and bone. Significantly greater birefringence per high-power microscopic field was observed among experimental specimens at fourteen, twenty-eight, and forty-two days compared with controls (C) (picrosirius red, ×320). *$p < 0.05$. **$p < 0.01$. T = tendon, B = bone, and IF = interface.

high-power field at three days to a peak of 1.5 ± 0.5 cells per high-power field at twenty-eight days.

There were significantly fewer ED1+ and ED2+ macrophages in the specimens from the macrophage-depleted limbs compared with the control limbs ($p < 0.05$ for ED1+ at all time points; $p < 0.01$ for ED2+ at three days, and $p < 0.05$ at all other times). Following serial injections of liposomal clodronate, the number of ED1+ macrophages at the tendon-bone interface of experimental animals remained constant, averaging 1.8 ± 0.6 cells per high-power field (range, 1.6 ± 0.9 to 2.1 ± 0.9 cells per high-power field) over all time points. This reflected a relative reduction in ED1+ cells of 82% at seven days, the point of peak ED1+ macrophage infiltration among control animals. Similarly, the number of ED2+ interface macrophages observed among treated specimens was constant at 0.1 ± 0.1 cells per high-power field (range, 0.04 ± 0.1 to 0.2 ± 0.1 cells per high-power field) over all time points. The reduction in ED2+ macrophages relative to control specimens ranged from 63% at three days to 85% at twenty-eight days.

TGF-β Staining at the Healing Tendon-Bone Interface

TGF-β-positive cells were found in the early inflammatory cell infiltrate at the tendon graft-bone interface at all time points. There was positive staining for TGF-β in vascular cells and fibroblasts in the tendon-bone interface. Compared with the control limbs, the macrophage-depleted specimens had significantly less TGF-β staining at every time point except seven days (6.2 ± 1.5 cells per high-power field and 2.1 ± 0.6 cells per high-power field, respectively, at fourteen days; 8.1 ± 0.9 cells per high-power field and 3.1 ± 1.9 cells per high-power field at twenty-eight days; and 6.9 ± 0.9 cells per high-power field and 4.2 ± 1.2 cells per high-power field at forty-two days; $p < 0.01$ for all) (Fig. 2).

Fibrous Tissue Formation and Remodeling at the Healing Tendon-Bone Interface

Healing between the tendon graft and bone tunnel in control specimens was initiated by the formation of a loose, poorly organized fibrous interface tissue. The interface consisted predominantly of neutrophils, fibroblasts, and mononuclear cells at the earliest time point, with only sparse collagen fibers within the matrix and distinct margins between tendon graft, interface, and bone. There were numerous islands of fragmented bone surrounding the interface along the tunnel. At seven days, the dominant cell morphology consisted of spindle-shaped fibroblasts. Osteoblasts were intermittently seen along

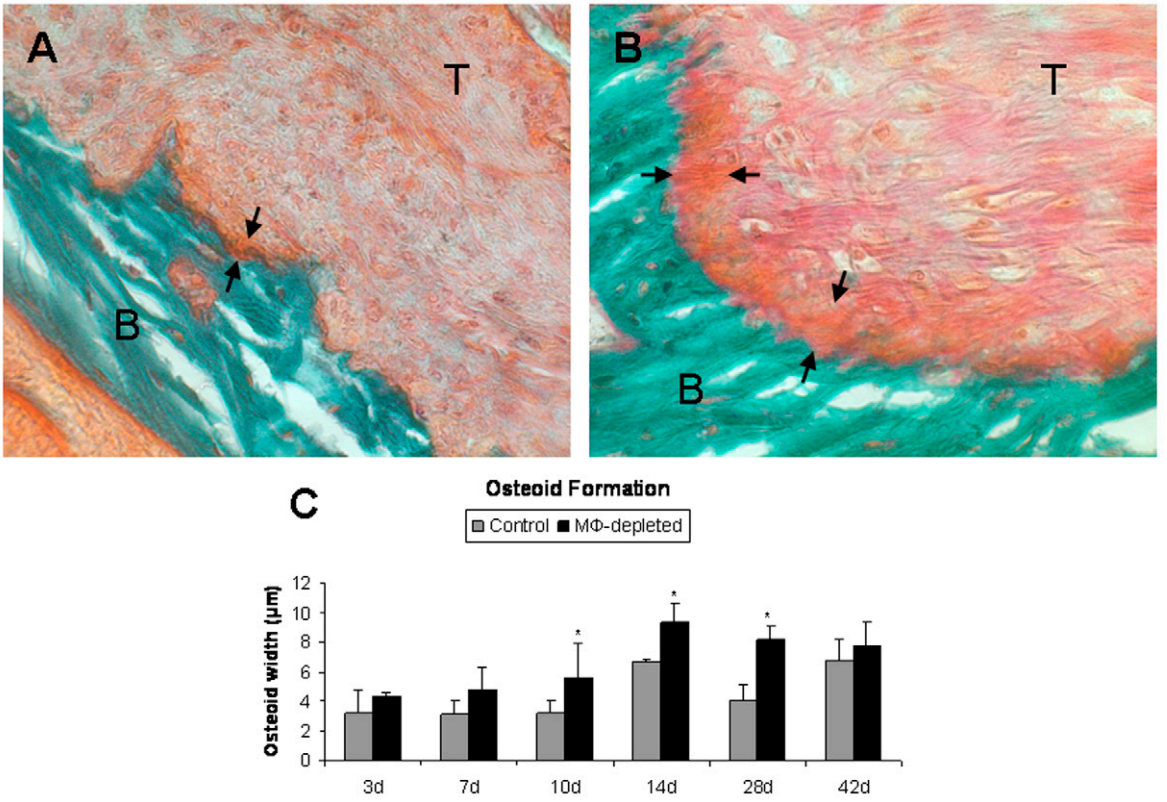

Fig. 5

At twenty-eight days, compared with controls (A), the specimens from animals that had been administered liposomal clodronate (B) demonstrated a significant increase in osteoid formation (arrows) at the tendon-bone interface. Macrophage depletion led to greater osteoid width compared with control specimens at all time points (C) (Goldner-Masson trichrome, ×320). *$p < 0.05$. T = tendon, and B = bone.

the edge of the bone tunnel. By ten days, there was increasing evidence of newly formed trabecular bone along the tendon-bone interface, and the fibrovascular interface tissue became denser and better organized, with evidence of early remodeling around the outer edge of the tendon graft. At fourteen days, increasing numbers of collagen fibers were observed aligning circumferentially around the bone tunnel. Occasional plump, round chondroid-appearing cells were also seen among the fibroblasts. By twenty-eight days, the interface tissue had a variable width among control specimens consisting of different degrees of remodeling, from dense fibrovascular tissue to less frequent areas of early fibrocartilage and collagen fiber continuity with bone. There were also increased numbers of osteoblasts along the bone tunnel with increased trabecular bone surrounding the interface. This pattern of healing continued to progress through forty-two days with more consistent areas of tissue remodeling and the increased presence of collagen fibers extending between the interface and bone.

Tendon-to-bone healing among the macrophage-depleted specimens progressed similarly to that of the control specimens but at an accelerated rate and with more marked interface remodeling, reestablishment of collagen fiber continuity, and direct bone ingrowth into tendon. At all time points, the width of the fibrous interface tissue measured between tendon graft and bone was significantly reduced among experimental limbs compared with controls (Figs. 3-A and 3-B). Three days following surgery, the relative reduction in interface tissue observed between groups was 48% (74.5 ± 13.3 μm compared with 38.8 ± 20.6 μm; $p < 0.01$). At seven days, additional differences between control and experimental specimens were evident. Tendon graft, interface, and bone tissues remained distinctly separate, but a more consistent perimeter of trabecular bone surrounded the grafts in the experimental group. Randomly dispersed collagen fibers were seen within the fibrous interface tissue, and there was a significant difference in interface width between control and experimental animals (116.5 ± 29.5 μm and 23.7 ± 7.1 μm, respectively; $p < 0.05$). At ten days, the healing interface in the macrophage-depleted group was characterized by a dense fibrovascular tissue with occasional large, round cells resembling chondrocytes. By fourteen days, distinct areas of collagen fiber continuity between tendon and bone had developed among all macrophage-depleted specimens. Occasional zones of early fibrocartilaginous tissue were seen in addition to an increased quantity of collagen fiber bundles bridging the

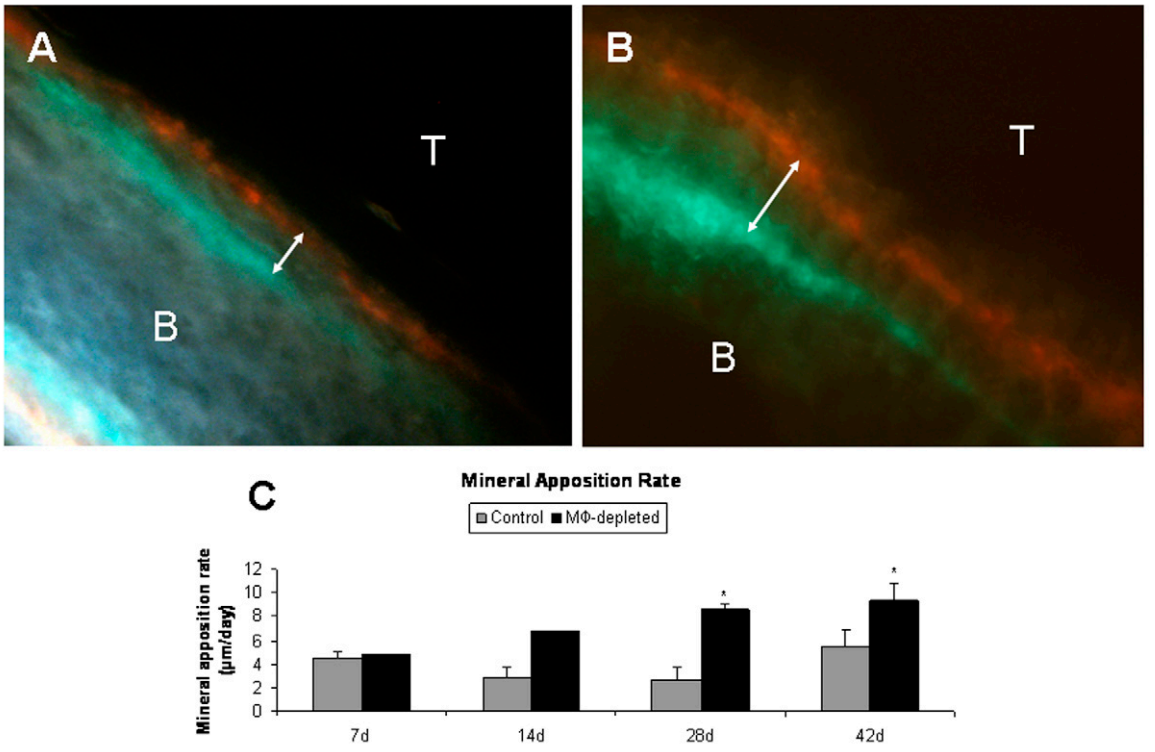

Fig. 6

At forty-two days, compared with the controls (A), the experimental specimens (B) had a greater distance between fluorochrome bone labels (arrows) (×320). The calculated rate of mineral apposition among macrophage-depleted animals was higher than that of controls at all time points with a significant difference at twenty-eight and forty-two days (C). *$p < 0.05$. T = tendon, and B = bone.

tendon graft and bone at 45° angles. The reduction in interface width between groups remained significant at ten and fourteen days (106.5 ± 29.8 μm compared with 30.7 ± 3.1 μm, and 124.5 ± 29.1 μm compared with 18.2 ± 5.8 μm, respectively; $p < 0.01$).

Healing continued to progress through twenty-eight days at which time the degree of interface remodeling among macrophage-depleted animals was significantly improved compared with controls (interface width of 135.5 ± 18.1 μm and 20.4 ± 4.9 μm, respectively; $p < 0.01$). Occasional areas of fibrovascular tissue were observed, but the interface morphology more commonly demonstrated a gradual transition between tendon graft and bone with early characteristics of a direct, four-zone insertion site. Increased numbers of collagen fibers resembling Sharpey fibers continued to align into the surrounding bone tunnel. By forty-two days, the quality of the tendon-bone interface among experimental sections consistently improved (interface width of 93.0 ± 11.2 μm compared with 18.4 ± 6.9 μm; $p < 0.01$).

Collagen Fiber Continuity at the Healing Tendon-Bone Interface

There was progressive establishment of collagen fiber continuity between tendon graft and bone tunnel among both groups following anterior cruciate ligament reconstruction. Under polarized light at high magnification, the presence of collagen fibers was recorded as mean birefringence per high-power field (Fig. 4). At seven days, poorly organized, sparse collagen fibers were identified at the tendon-bone interface in the control specimens, and only limited bundles of collagen fibers were present along the perimeter of the bone tunnel by fourteen days. The degree of collagen fiber continuity among control animals continued to increase at twenty-eight and forty-two days with steady improvements in fiber organization and alignment.

In contrast, there was more rapid establishment of collagen fiber continuity in the macrophage-depleted animals compared with the controls at fourteen, twenty-eight, and forty-two days. Similar to the control specimens, the macrophage-depleted animals had birefringent areas of collagen fibers at seven days, but they remained relatively unorganized and only intermittently distributed along the interface. At fourteen days, the mean birefringence observed at the interface of experimental specimens was significantly greater than that of controls ($p < 0.05$). Markedly increased and more consistent collagen fiber continuity was also present at twenty-eight and forty-two days among the experimental animals compared with controls ($p < 0.01$).

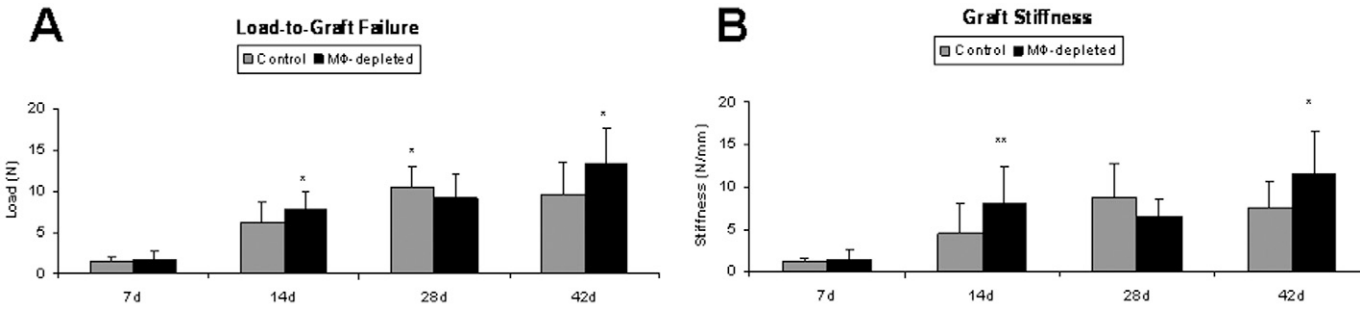

Fig. 7

Load-to-graft failure (A) and graft stiffness (B) were greater among macrophage-depleted specimens at seven and fourteen days. By twenty-eight days, control specimens demonstrated improved biomechanical properties compared with experimental specimens. At forty-two days following anterior cruciate ligament reconstruction, the macrophage depletion group again had significantly higher failure load and stiffness compared with controls. *$p < 0.05$. **$p < 0.01$.

New Bone Formation at the Healing Tendon-Bone Interface

Newly formed osteoid was observed along the bone tunnels of control and experimental animals at all time points. New bone formation remained relatively constant from three to ten days among control animals (3.1 ± 0.9 μm to 3.2 ± 1.6 μm, respectively) and liposomal clodronate-treated animals (4.4 ± 0.2 μm to 5.6 ± 2.3 μm; $p < 0.05$ for the difference between groups at ten days), with greater widths of new bone forming along the bone tunnels of experimental limbs (Fig. 5). At fourteen days, an increase in osteoid formation was observed among both control and macrophage-depleted groups (6.6 ± 0.2 μm and 9.3 ± 1.2 μm, respectively; $p < 0.05$), and a significantly greater width of osteoid was also seen among macrophage-depleted animals at twenty-eight days (4.1 ± 1.0 μm and 8.2 ± 0.9 μm, respectively; $p < 0.05$). By forty-two days, osteoid formation along the bone tunnel remained high (6.8 ± 1.4 μm for controls compared with 7.8 ± 1.5 μm for the experimental group), but no significant difference was observed between groups.

The mineral apposition rate was determined at seven, fourteen, twenty-eight, and forty-two days by serial fluorochrome labeling of bone observed under fluorescent light. Uptake of one or both of the fluorochromes was inconsistent at seven and fourteen days, limiting the number of specimens available for statistical analysis. Nonetheless, trends were consistent with those observed for new osteoid formation. At seven days, the rates of bone mineralization were similar between control and experimental groups (4.5 ± 0.5 μm/day and 4.9 μm/day, respectively; Fig. 6). An increased mineral apposition rate among macrophage-depleted animals was observed at all other time points, with significant differences compared with controls at twenty-eight and forty-two days (2.9 ± 0.9 μm/day and 6.8 μm/day, respectively, at fourteen days; 2.6 ± 1.1 μm/day and 8.6 ± 0.5 μm/day at twenty-eight days, $p < 0.05$; and 5.5 ± 1.4 μm/day and 9.4 ± 1.4 μm/day at forty-two days, $p < 0.05$).

Biomechanical Testing

Of ninety-six specimens, ten were discarded as a result of either graft failure discovered at the time of killing (one control and three experimental animals) or inadequate dissection leading to inaccurate load and stiffness values (three control and three experimental animals). These animals were not replaced.

Among control specimens, load to failure and stiffness increased significantly from seven to fourteen days ($p < 0.01$; Fig. 7) and from fourteen to twenty-eight days ($p < 0.01$). Between twenty-eight and forty-two days, there was no significant change in load to failure and stiffness among control animals. Similarly, a significant increase in load and stiffness was observed among macrophage-depleted limbs between seven and fourteen days ($p < 0.01$) and between twenty-eight and forty-two days ($p < 0.01$), but not between fourteen and twenty-eight days.

At seven days, the control and experimental groups had similar findings with respect to load to failure (1.5 ± 0.7 N and 1.6 ± 1.0 N, respectively) and stiffness (1.1 ± 0.5 N/mm and 1.6 ± 1.1 N/mm). At fourteen days, a significant increase was observed among macrophage-depleted limbs compared with the controls with regard to both load to failure (7.9 ± 2.1 N and 6.1 ± 2.6 N; $p < 0.05$) and stiffness (8.0 ± 4.4 N/mm and 4.5 ± 3.4 N/mm; $p < 0.01$). At twenty-eight days, the control specimens exhibited significant increases compared with macrophage-depleted limbs with respect to mean load (10.5 ± 2.4 N and 9.2 ± 2.8 N, respectively; $p < 0.05$) and mean stiffness (8.7 ± 4.1 N/mm and 6.5 ± 2.0 N/mm). By forty-two days, experimental animals again had significant increases compared with the controls with respect to mean load to failure (13.5 ± 4.2 N and 9.7 ± 3.9 N, respectively; $p < 0.05$) and mean stiffness (11.5 ± 5.0 N/mm and 7.5 ± 3.2 N/mm; $p < 0.05$).

The failure mode during biomechanical testing was recorded as tunnel pullout, tendon midsubstance failure, or combined pullout and midsubstance failure (Table I). The pattern of graft failure was similar between the groups. The mode of failure observed in both groups at seven and fourteen days, which was predominantly by graft pullout, was significantly different from that at twenty-eight and forty-two days, which more commonly involved either complete or partial failure at the midsubstance of the tendon (chi-square test; $p < 0.05$).

TABLE I Type of Failure Mode Recorded During Biomechanical Testing

Group	Tunnel Pullout	Tendon Graft Midsubstance Failure	Combined Tunnel Pullout and Midsubstance Failure
7 days			
Control	9	0	0
Experimental	8	0	0
14 days			
Control	10	0	1
Experimental	12	0	0
28 days			
Control	3	5	4
Experimental	0	7	5
42 days			
Control	0	7	5
Experimental	1	6	3

Discussion

In this study, we used a rat model of anterior cruciate ligament reconstruction to study healing of a tendon graft in a bone tunnel. We developed this model to take advantage of the availability of rat-specific molecular and immunohistochemical reagents. Our previous work with this model characterized the inflammatory cell infiltrate that is present in the early healing period and suggested the important role of macrophages in the early healing process between tendon and bone[11]. Since studies by us and others have shown that there is formation of a "scar tissue" interface between tendon and bone rather than reformation of a normal insertion site, we hypothesized that the presence of abundant macrophages plays an important role in this scar formation. In other experimental models, the presence of macrophages and overexpression of TGF-β has been linked to states of chronic inflammation and tissue fibrosis[14,15,21,25,28,30,31]. In contrast, embryonic wounds heal in the absence of an inflammatory cell infiltrate with recapitulation of normal, "scar-less" tissue morphology. Studies of macrophage depletion have demonstrated substantial reductions in the degree of fibrosis as well as accelerated tissue healing[14,19,39,40]. Moreover, inhibition of TGF-β in wounds has been shown to reduce tissue fibrosis[14,27,28], while overexpression results in a chronic fibrotic state[15,21,31].

We selectively depleted macrophages using a liposome-encapsulated bisphosphonate, liposomal clodronate. Liposomal clodronate has been used by other investigators to demonstrate the antifibrotic and regenerative effects of macrophage depletion in models of organ fibrosis[32,40,41]. The effects of liposomal clodronate on macrophages have been shown to last for two weeks following administration[42]. To our knowledge, this is the first study to examine the effect of macrophage depletion on tendon-to-bone healing in a ligament reconstruction model.

Healing at the tendon-bone interface in this model begins with an early inflammatory cell infiltrate, followed by formation of a loose, poorly organized fibrous tissue interface. As healing proceeds, there is gradual bone ingrowth into tendon and progressive reestablishment of collagen fiber continuity between interface and bone. We did not find consistent reformation of a native ligament insertion morphology, with a fibrocartilage transition zone between ligament and bone. The pattern of macrophage infiltration at the tendon graft-bone tunnel interface in our control specimens was similar to that in a previous study in our laboratory[11]. ED1+ macrophages, recruited from circulating blood monocytes, were present by three days following surgery, peaked around seven days, and subsequently declined in number. ED2+ cells, derived from the local tissue environment, accumulated in smaller numbers by seven days and peaked by twenty-eight days. Among animals administered liposomal clodronate, the numbers of ED1+ and ED2+ macrophages were significantly reduced at all time points through forty-two days ($p < 0.05$), with a decrease in total cell number ranging from 56% to 87% for ED1+ cells and 63% to 85% for ED2+ cells.

Tendon-to-bone healing among experimental (macrophage-depleted) animals proceeded at an accelerated rate compared with untreated control specimens, with significantly reduced formation of loose, fibrovascular tissue and earlier tissue organization; closer apposition of tendon graft to bone; and an increase in the number and size of collagen fiber bundles resembling Sharpey fibers that were perpendicularly aligned at the tendon-bone interface as early as fourteen days following surgery. Bone formation as measured by newly forming osteoid along the perimeter of the bone tunnel was significantly increased in macrophage-depleted animals at fourteen and twenty-eight days, suggesting increased activity at the bone tunnel with enhanced bone ingrowth into tendon. Furthermore, by twenty-eight days, areas of remodeling fibrocartilage extending from the bone tunnel to the graft were observed among macrophage-depleted animals, suggesting partial reestablishment of a healing morphology more similar to that of a native enthesis. At forty-two days, distinct areas of fibrocartilage transition from tendon to bone similar to the zonal pattern of native attachment sites were more often observed with consistent reestablishment of collagen fiber continuity between tendon and bone. These morphologic changes resulted in significant improvements in biomechanical load to failure and graft stiffness compared with controls by forty-two days.

The formation of fibrous scar tissue at the healing tendon-bone interface is the result of extracellular matrix production by activated fibroblasts. The extent of extracellular matrix deposition and fibrosis is largely under the influence of macrophage-mediated cytokine production. Following tissue injury, platelet degranulation releases macrophage chemoattractants including TGF-β. This early population of macrophages recruited from circulating blood monocytes undergoes "classical activation"[39,40,43,44]. These macrophages function in débridement of the local tissue environment and phagocytosis of apoptotic inflammatory cells. Classically activated macro-

phages release proinflammatory cytokines such as interleukin (IL)-1, IL-6, and TNF-α as well as matrix proteases, which aid in cell chemotaxis through the inflammatory milieu. Prior studies have shown that macrophage phagocytosis of apoptotic cells results in a phenotypic transition from "classical" to "alternative" activation[39]. Alternatively activated macrophages, in contrast, release anti-inflammatory and profibrogenic cytokines. These cells produce TGF-β and platelet-derived growth factor and contribute to myofibroblast activation and proliferation, resulting in increased extracellular matrix synthesis, remodeling, and scar formation.

The balance between matrix remodeling and excessive fibrosis and the roles of macrophages in these processes is complex and incompletely understood. We found diminished TGF-β expression in concert with diminished macrophage numbers. The role of cytokines in tissue healing is complex and dependent on numerous factors, including the timing of application, concentration, and the cell types present. For example, a number of studies have suggested that exogenously applied TGF-β may enhance healing, extracellular matrix synthesis, and remodeling[15,23,45,46]. Yamazaki et al. recently described the effects of exogenously applied TGF-β on tendon-bone healing in a canine model of anterior cruciate ligament reconstruction[46]. In that study, the TGF-β-treated grafts demonstrated increased load and stiffness over the fibrin glue and negative controls as well as increased collagen fiber synthesis and new bone formation along the tunnel. These effects were due to increased formation of fibrous scar tissue in the tendon-bone interface. These results support our hypothesis that macrophage-derived cytokines, such as TGF-β, lead to reactive scar-tissue formation at the healing tendon-bone junction. Even though the addition of TGF-β enhanced tendon-bone healing in the described study, healing was "improved" only by formation of a greater quantity of scar tissue, which likely has inferior material properties compared with a normal insertion site. Our hypothesis is that blocking of the excessive inflammatory response allows expression of "innate" healing mechanisms and regeneration of a more normal insertion site rather than reactive scar formation.

The role of macrophages in wound-healing is complex, and we acknowledge that alteration of macrophage numbers is likely to have myriad effects on healing. Macrophages present during the early inflammatory phase of healing that produce proinflammatory mediators may have a negative effect on tissue regeneration. In the present study, we suggest that macrophage depletion led to abrogation of the early "destructive" phase of inflammatory healing, perhaps allowing expression of genes appropriate for tissue regeneration rather than reactive scar formation. Activated myofibroblasts and neutrophils likely compensated for the phagocytic responsibilities typically performed by macrophages[29].

However, macrophages play an important role in the resolution of inflammation by phagocytosis of apoptotic neutrophils before these cells lyse. Resolution of inflammation is necessary for a healing wound to progress to matrix synthesis and maturation, and it contributes to the activation of macrophages with a reparative phenotype[47-50]. The cytokine profile in the healing wound also changes as inflammation resolves. For example, Dahlgren et al. studied growth factor expression in tendon healing and found an early peak of TGF-β1 at one week, coinciding with the early proinflammatory period[51]. Of particular interest, this group suggests that inhibition of early TGF-β1 expression could result in downregulation of the inflammatory cytokine environment, allowing earlier expression of insulin-like growth factor (IGF)-I (which has a strong positive role in tendon healing) in its restorative and pro-regenerative capacities. A similar mechanism may explain our results, as macrophage depletion diminished TGF-β1 expression, which may permit earlier IGF-I activity and accelerate regenerative healing of tendon to bone.

Further study is required to determine whether healing can be improved by selective inhibition of only the earliest proinflammatory macrophage phenotype. It is unknown whether it is possible to "uncouple" the early proinflammatory and late reparative macrophage populations. It is possible that the induction-autoinduction mechanisms are so interdependent that knocking out early macrophages would by default impair their late regenerative activity.

Although the improved biomechanical results in the controls at twenty-eight days may simply be due to biologic variability, consideration of the role of reparative macrophage populations in the later phases of healing suggests a possible mechanism to explain this reversal in the biomechanical results. The presence of such reparative macrophages and associated cytokines in the healing environment in the control animals may lead to increased fibrous tissue formation and thus improved attachment strength. However, we hypothesize that there is a limit to the ultimate attachment strength of this fibrous scar-tissue interface. The closer apposition of tendon and bone in the macrophage-depleted animals (due to less scar tissue in the interface) may allow for continued development of collagen fiber continuity and ultimately a stronger attachment. However, this is currently speculative and further study is required to test this proposed mechanism.

Alteration of macrophage numbers may also affect healing through an effect on matrix metalloproteinases (MMPs) and their inhibitors (tissue inhibitors of metalloproteinases [TIMPs]). The balance between extracellular matrix synthesis and degradation is closely related to the activities of these molecules[52-54]. Macrophages are known to produce MMPs and TIMPs[52,53]. In a recent study, Demirag et al. studied the effects of synovial matrix metalloproteinase activity on tendon-bone healing using α_2-macroglobulin as an MMP-blocking agent in a rabbit model of anterior cruciate ligament reconstruction[55]. They found that, following treatment with α_2-macroglobulin, the specimens had decreased postoperative enzymatic activity and improved graft-healing with enhanced collagen fiber continuity and biomechanical strength. Considering this evidence, it is possible in the present study that depletion of macrophages following anterior cruciate ligament reconstruction may have altered the levels of early postinjury MMPs and their relative balance with other cytokines, leading to reduced col-

lagenase-mediated matrix destruction and enhancement of tendon graft-healing.

Our study has several limitations. We evaluated animals only to forty-two days after surgery. However, our previous work demonstrated that the early inflammatory phase and the phase of cellular and matrix proliferation are largely resolved by forty-two days in the rat model. Further study is required to examine the effect of macrophage depletion on late remodeling. Further study is also required to elucidate the complex functions of macrophages, their role in tendon healing, and the interaction between mechanical load on the healing tendon-bone interface and macrophage activity. Another important consideration is that osteoclasts are derived from cells closely related to (if not the same as) the precursors of macrophages. As a result, besides depleting macrophages, our clodronate-loaded liposomes may have also had an effect on osteoclasts. Some of the differences in remodeling and mineralization could reflect an inhibition of osteoclasts. Another limitation is that we did not use a control group that received liposomes without clodronate; however, there is no evidence that the liposomes alone would have any effect on healing.

In conclusion, the results of this study suggest that macrophage depletion enhances tendon-to-bone healing in a rat model of anterior cruciate ligament reconstruction. We found changes in the structural, compositional, and biomechanical properties of the healing tendon-bone interface. Healing of a tendon graft in a bone tunnel in macrophage-depleted animals progressed at an accelerated rate on the basis of the reestablishment of collagen fiber continuity, new bone formation, and the overall degree of interface remodeling. There was less fibrous tissue (scar) formation at the healing tendon-bone interface, perhaps because of decreased expression of TGF-β. Likewise, biomechanical properties of load-to-graft failure and graft stiffness were significantly improved at forty-two days with macrophage depletion. Clearly, the process of tendon-to-bone healing is complex, with multiple simultaneous and compensatory pathways governing early postoperative remodeling. These findings suggest the need for further study of the role of macrophages in tendon-to-bone healing in a large animal model to further delineate the cellular and molecular mechanisms of healing. ■

NOTE: The authors thank David Kovacevic, BS, for assistance with the statistical analyses and final manuscript preparation.

Peyton L. Hays, MD
Sumito Kawamura, MD
Xiang-Hua Deng, MD
Elias Dagher, MD
Kai Mithoefer, MD
Liang Ying, BS
Scott A. Rodeo, MD
The Hospital for Special Surgery, 535 East 70th Street, New York, NY 10021. E-mail address for S.A. Rodeo: rodeos@hss.edu

References

1. Gordon MD, Steiner ME. Anterior cruciate ligament injuries. In: Garrick JG, editor. Orthopaedic knowledge update: sports medicine 3. Rosemont, IL: American Academy of Orthopaedic Surgeons; 2004. p 169-81.

2. Beynnon BD, Johnson RJ, Fleming BC, Kannus P, Kaplan M, Samani J, Renström P. Anterior cruciate ligament replacement: comparison of bone-patellar tendon-bone grafts with two-strand hamstring grafts. A prospective, randomized study. J Bone Joint Surg Am. 2002;84:1503-13.

3. Barber-Westin SD, Noyes FR, Heckmann TP, Shaffer BL. The effect of exercise and rehabilitation on anterior-posterior knee displacements after anterior cruciate ligament autograft reconstruction. Am J Sports Med. 1999;27:84-93.

4. Howell SM, Taylor MA. Brace-free rehabilitation, with early return to activity, for knees reconstructed with a double-looped semitendinosus and gracilis graft. J Bone Joint Surg Am. 1996;78:814-25.

5. Shelbourne KD, Whitaker HJ, McCarroll JR, Rettig AC, Hirschman LD. Anterior cruciate ligament injury: evaluation of intraarticular reconstruction of acute tears without repair. Two to seven year followup of 155 athletes. Am J Sports Med. 1990;18:484-9.

6. Sharma P, Maffulli N. Tendon injury and tendinopathy: healing and repair. J Bone Joint Surg Am. 2005;87:187-202.

7. Panni AS, Milano G, Lucania L, Fabbriciani C. Graft healing after anterior cruciate ligament reconstruction in rabbits. Clin Orthop Relat Res. 1997;343:203-12.

8. Evans CH. Cytokines and the role they play in the healing of ligaments and tendons. Sports Med. 1999;28:71-6.

9. Grana WA, Egle DM, Mahnken R, Goodhart CW. An analysis of autograft fixation after anterior cruciate ligament reconstruction in a rabbit model. Am J Sports Med. 1994;22:344-51.

10. Kawamura S, Hays P, Mithoefer K, Sussmann PS, Ying L, Rodeo SA. Macrophage depletion affects healing of a tendon graft in a bone tunnel. Trans Orthop Res Soc. 2005;30:412. Poster no. 0412.

11. Kawamura S, Ying L, Kim HJ, Dynybil C, Rodeo SA. Macrophages accumulate in the early phase of tendon-bone healing. J Orthop Res. 2005;23:1425-32.

12. Rodeo SA, Arnoczky SP, Torzilli PA, Hidaka C, Warren RF. Tendon-healing in a bone tunnel. A biomechanical and histological study in the dog. J Bone Joint Surg Am. 1993;75:1795-803.

13. Rodeo SA, Suzuki K, Deng XH, Wozney J, Warren RF. Use of recombinant human bone morphogenetic protein-2 to enhance tendon healing in a bone tunnel. Am J Sports Med. 1999;27:476-88.

14. Choi BM, Kwak HJ, Jun CD, Park SD, Kim KY, Kim HR, Chung HT. Control of scarring in adult wounds using antisense transforming growth factor-beta 1 oligodeoxynucleotides. Immunol Cell Biol. 1996;74:144-50.

15. Connors D, Gies D, Lin H, Gruskin E, Mustoe TA, Tawil NJ. Increase in wound breaking strength in rats in the presence of positively charged dextran beads correlates with an increase in endogenous transforming growth factor-beta1 and its receptor TGF-betaRI in close proximity to the wound. Wound Repair Regen. 2000;8:292-303.

16. Frangogiannis NG, Smith CW, Entman ML. The inflammatory response in myocardial infarction. Cardiovasc Res. 2002;53:31-47.

17. Erwig LP, Kluth DC, Walsh GM, Rees AJ. Initial cytokine exposure determines function of macrophages and renders them unresponsive to other cytokines. J Immunol. 1998;161:1983-8.

18. Marsolais D, Côté CH, Frenette J. Neutrophils and macrophages accumulate sequentially following Achilles tendon injury. J Orthop Res. 2001;19:1203-9.

19. Wolff RA, Tomas JJ, Hullett DA, Stark VE, van Rooijen N, Hoch JR. Macrophage depletion reduces monocyte chemotactic protein-1 and transforming growth factor-beta1 in healing rat vein grafts. J Vasc Surg. 2004;39:878-88.

20. Barnard JA, Lyons RM, Moses HL. The cell biology of transforming growth factor beta. Biochim Biophys Acta. 1990;1032:79-87.

21. Border WA, Ruoslahti E. Transforming growth factor-beta in disease: the dark side of tissue repair. J Clin Invest. 1992;90:1-7.

22. Chegini N. The role of growth factors in peritoneal healing: transforming growth factor beta (TGF-beta). Eur J Surg Suppl. 1997;577:17-23.

23. Ignotz RA, Massague J. Transforming growth factor-beta stimulates the expression of fibronectin and collagen and their incorporation into the extracellular matrix. J Biol Chem. 1986;261:4337-45.

24. Shull MM, Ormsby I, Kier AB, Pawlowski S, Diebold RJ, Yin M, Allen R, Sidman C, Proetzel G, Calvin D, Annunziata N, Doetschman T. Targeted disruption of the mouse transforming growth factor-β1 gene results in multifocal inflammatory disease. Nature. 1992;359:693-9.

25. Hopkinson-Woolley J, Hughes D, Gordon S, Martin P. Macrophage recruitment during limb development and wound healing in the embryonic and foetal mouse. J Cell Sci. 1994;107:1159-67.

26. Whitby DJ, Ferguson MW. Immunohistochemical localization of growth factors in fetal wound healing. Dev Biol. 1991;147:207-15.

27. Ashcroft GS, Yang X, Glick AB, Weinstein M, Letterio JL, Mizel DE, Anzano M, Greenwell-Wild T, Wahl SM, Deng C, Roberts AB. Mice lacking Smad3 show accelerated wound healing and an impaired local inflammatory response. Nat Cell Biol. 1999;1:260-6.

28. Shah M, Foreman DM, Ferguson MW. Control of scarring in adult wounds by neutralising antibody to transforming growth factor beta. Lancet. 1992;339:213-4.

29. Martin P, D'Souza D, Martin J, Grose R, Cooper L, Maki R, McKercher SR. Wound healing in the PU.1 null mouse—tissue repair is not dependent on inflammatory cells. Curr Biol. 2003;13:1122-8.

30. Harty M, Neff AW, King MW, Mescher AL. Regeneration or scarring: an immunologic perspective. Dev Dyn. 2003;226:268-79.

31. Lin RY, Sullivan KM, Argenta PA, Meuli M, Lorenz HP, Adzick NS. Exogenous transforming growth factor-beta amplifies its own expression and induces scar formation in a model of human fetal skin repair. Ann Surg. 1995;222:146-54.

32. Zhang-Hoover J, Sutton A, van Rooijen N, Stein-Streilein J. A critical role for alveolar macrophages in elicitation of pulmonary immune fibrosis. Immunology. 2000;101:501-11.

33. Van Rooijen N, Sanders A. Liposome mediated depletion of macrophages: mechanism of action, preparation of liposomes and applications. J Immunol Methods. 1994;174:83-93.

34. Wu G, Korsgren O, Zhang J, Song Z, van Rooijen N, Tibell A. Pig islet xenograft rejection is markedly delayed in macrophage-depleted mice: a study in streptozotocin diabetic animals. Xenotransplantation. 2000;7:214-20.

35. Dijkstra CD, Döpp EA, Joling P, Kraal G. The heterogeneity of mononuclear phagocytes in lymphoid organs: distinct macrophage subpopulations in the rat recognized by monoclonal antibodies ED1, ED2 and ED3. Immunology. 1985;54:589-99.

36. Honda H, Kimura H, Rostami A. Demonstration and phenotypic characterization of resident macrophages in rat skeletal muscle. Immunology. 1990;70:272-7.

37. Junqueira LCU, Bignolas G, Brentani RR. Picrosirius staining plus polarization microscopy, a specific method for collagen detection in tissue sections. Histochem J. 1979;11:447-55.

38. Pickering JG, Boughner DR. Quantitative assessment of the age of fibrotic lesions using polarized light microscopy and digital image analysis. Am J Pathol. 1991;138:1225-31.

39. Duffield JS. The inflammatory macrophage: a story of Jekyll and Hyde. Clin Sci (Lond). 2003;104:27-38.

40. Duffield JS, Forbes SJ, Constandinou CM, Clay S, Partolina M, Vuthoori S, Wu S, Lang R, Iredale JP. Selective depletion of macrophages reveals distinct, opposing roles during liver injury and repair. J Clin Invest. 2005;115:56-65.

41. van Rooijen N, Sanders A. Elimination, blocking, and activation of macrophages: three of a kind? J Leukoc Biol. 1997;62:702-9.

42. Hoch JR, Stark VK, van Rooijen N, Kim JL, Nutt MP, Warner TF. Macrophage depletion alters vein graft intimal hyperplasia. Surgery. 1999;126:428-37.

43. Goerdt S, Orfanos CE. Other functions, other genes: alternative activation of antigen-presenting cells. Immunity. 1999;10:137-42.

44. Song E, Ouyang N, Hörbelt M, Antus B, Wang M, Exton MS. Influence of alternatively and classically activated macrophages on fibrogenic activities of human fibroblasts. Cell Immunol. 2000;204:19-28.

45. Sumner DR, Turner TM, Purchio AF, Gombotz WR, Urban RM, Galante JO. Enhancement of bone ingrowth by transforming growth factor-beta. J Bone Joint Surg Am. 1995;77:1135-47.

46. Yamazaki S, Yasuda K, Tomita F, Tohyama H, Minami A. The effect of transforming growth factor-beta1 on intraosseous healing of flexor tendon autograft replacement of anterior cruciate ligament in dogs. Arthroscopy. 2005;21:1034-41.

47. Fadok VA, Bratton DL, Konowal A, Freed PW, Westcott JY, Henson PM. Macrophages that have ingested apoptotic cells in vitro inhibit proinflammatory cytokine production through autocrine/paracrine mechanisms involving TGF-beta, PGE2, and PAF. J Clin Invest. 1998;101:890-8.

48. McDonald PP, Fadok VA, Bratton D, Henson PM. Transcriptional and translational regulation of inflammatory mediator production by endogenous TGF-beta in macrophages that have ingested apoptotic cells. J Immunol. 1999;163:6164-72.

49. Daley JM, Reichner JS, Mahoney EJ, Manfield L, Henry WL Jr, Mastrofrancesco B, Albina JE. Modulation of macrophage phenotype by soluble product(s) released from neutrophils. J Immunol. 2005;174:2265-72.

50. Murai N, Nagai K, Fujisawa H, Hatanaka K, Kawamura M, Harada Y. Concurrent evolution and resolution in an acute inflammatory model of rat carrageenin-induced pleurisy. J Leukoc Biol. 2003;73:456-63.

51. Dahlgren LA, Mohammed HO, Nixon AJ. Temporal expression of growth factors and matrix molecules in healing tendon lesions. J Orthop Res. 2005;23:84-92.

52. Foos MJ, Hickox JR, Mansour PG, Slauterbeck JR, Hardy DM. Expression of matrix metalloprotease and tissue inhibitor of metalloprotease genes in human anterior cruciate ligament. J Orthop Res. 2001;19:642-9.

53. Ma C, Tarnuzzer RW, Chegini N. Expression of matrix metalloproteinases and tissue inhibitor of matrix metalloproteinases in mesothelial cells and their regulation by transforming growth factor-beta1. Wound Repair Regen. 1999;7:477-85.

54. Reno C, Boykiw R, Martinez ML, Hart DA. Temporal alterations in mRNA levels for proteinases and inhibitors and their potential regulators in the healing medial collateral ligament. Biochem Biophys Res Comm. 1998;252:757-63.

55. Demirag B, Sarisozen B, Ozer O, Kaplan T, Ozturk C. Enhancement of tendon-bone healing of anterior cruciate ligament grafts by blockage of matrix metalloproteinases. J Bone Joint Surg Am. 2005;87:2401-10.